Brazilian Dental Journal (2016) 27(3): 243-254
http://dx.doi.org/10.1590/0103-6440201602450

ISSN 0103-6440

Platelet Rich Plasma (PRP) Produces an Atherofibrotic Histophenotype During Craniofacial Bone Repair Due to Changes of Immunohistochemical Expression of Erk1/2, p38α/β, Adiponectin and Elevated Presence of Cells Exhibiting B-scavenger Receptor (CD36+)

Caroline Cristine Schroeder, Juliana Souza Vieira, Rafaela Scariot, João Cesar Zielak, Geraldo Monteiro Ribeiro, Tatiana Miranda Deliberador, Andrea M. Marcaccini, Allan Fernando Giovanini

Graduate Program in Dentistry, UP - Universidade Positivo, Curitiba, PR, Brazil

Correspondence: Dr. Allan Fernando Giovanini, Rua Pedro Viriato Parigot de Souza, 5300, 81280-330 Curitiba, PR, Brasil. Tel: +55-41-3317-3000. e-mail: afgiovanini@gmail.com

The platelet-extracellular matrix interaction in platelet rich plasma (PRP) through thrombospondin receptor-CD36 induces the secretion of growth factors responsible for cellular proliferation and differentiation during the repair process. Since CD36 also acts as a class B-scavenger-receptor for development of foam-like cells and mitogen-activated kinases, such as Erk1/2 and p38α/β, are important proteins activated by platelet growth factor, the aim of this study was to evaluate the immunohistochemical presence of CD36, Erk1/2, p38α/β during the bone repair treated and non-treated with PRP and to compare these results with the histomorphometry of repair. Simultaneously, the immunopresence of adiponectin was analyzed, which may contribute to osteogenesis at the same time it inhibits fibrosis and impairs adipogenesis and foam cell formation in the medullary area. An artificial bone defect measuring 5×1 mm was produced in the calvaria of 56 Wistar rats. The defects were randomly treated with autograft, autograft+PRP, PRP alone and sham. The animals were euthanized at 2 and 6 weeks post-surgery. Data were analyzed by ANOVA followed by non-parametric test Student Newman-Keuls ($p<0.05$) for histomorphometric and immunohistochemical interpretation. The results revealed that in specimens that received PRP the immunopositivity for Erk1/2, p38α/β and CD36 proteins increased significantly while the immunohistochemical expression of adiponectin decreased simultaneously. There was also an accentuated reduction of bone matrix deposition and increase of the medullary area represented by fibrosis and/or presence of foam-like cells, which exhibited immunophenotype CD36+adiponectin. The findings of this study suggest that PRP acted as an inhibitor of osteogenesis during the craniofacial bone repair and induced a pathological condition that mimics an atherofibrotic condition.

Key Words: bone regeneration, platelet-rich plasma, mitogen-activated program kinases, extracellular signal-regulated kinases-1/2 (Erk1/2), p38α/β, adiponectin, scavenger receptor CD36.

Introduction

Since Marx (1) described a larger and faster bone matrix formation in mandible using an autogenous blood fraction rich in platelets named platelet-rich plasma (PRP), this compound became a promising alternative for the treatment craniofacial bone defects due to its easy application in clinical practice and hypothetical beneficial results (2). The favorable use of PRP for osteogenesis has been substantiated on the hypothesis that the platelets produce growth factors that modulate the synthesis and deposition of extracellular matrix (ECM) and angiogenesis, and promotes chemotaxis of osteoprogenitor cells and their differentiation into osteoblasts (3). Nonetheless, despite this remarkable biological action, it has been claimed that the presence of PRP may not only impair osteogenesis, but also produce an abnormal histophenotype during craniofacial bone repair (4,5).

In fact, the main action of platelets is not directly correlated to osteogenesis. It is rather associated with the maintenance of post-injury hemostasis by the thrombi formed by the interaction between ECM-proteins and platelets. This condition induces platelet activation and is detected by the expression of anchorage molecules, especially the CD36 molecule (glycoprotein IV or thrombospondin receptor) (6). Once activated, EMC-adherent platelets produce chemokines and growth factors that are important to vascular and tissue formation and remodeling (7). However, CD36 is also known to be a class

B scavenger receptor, which, under pathological conditions, contributes directly to the formation of foam cells, as observed for example in dyslipidemia (8).

Bone matrix formation is a complex event whose final step is the production, maturation and mineralization of the ECM produced in injured bone sites (9). During bone matrix formation, the ECM cells usually recognize and respond to extracellular stimuli by intracellular signal programs that lead to the activation of mitogen-activated program kinases (MAPKs) (10). MAPKs may regulate cellular activities including mitosis, metabolism to motility and cellular differentiation inducing gene expression depending on the type of stimuli and tissue (11).

The extracellular signal-regulated kinases-1/2 (Erk1/2) and p38α/β are two MAPK proteins that act as transcription factors for some early genes, including proteins for osteoblast differentiation (12). On the other hand, Erk1/2 and p38α/β are also kinases co-expressed during platelet aggregation and they seem to be important for the formation of perivascular tunicae proliferation and differentiation or may contribute to pathological fibrosis. Additionally, Erk1/2 and p38α/β expression is mediated by Ser/Thr kinases pathways activated by TGF-β1, which is the main growth factor synthesized and released by activated platelets (13).

Adiponectin is a multifunctional plasmatic cell signaling protein secreted by adipose tissue (adipokine) that aids in the modulation of inflammation and tissue metabolism. Since adiponectin has a collagen-like N-terminal, this adipokine acts as an antithrombotic factor, minimizes fibrosis (14) and also contributes to the increase of bone mass and protection against dyslipidemia and foam cell formation, thus contributing to tissue homeostasis (15).

Thus the aim of this study was to evaluate the effect of PRP on the immunohistochemical expression of CD36, Erk1/2, p38α/β and adiponectin, and compare these results with the histomorphometry of bone matrix development produced during bone repair.

Material and Methods

Fifty-six 5-6-month-old male Wistar rats (*Rattus norvegicus albinus*) weighing 450 to 500 g and no previous disease were used following a protocol approved by the Institutional Board for Animal Care and Use. The rats were kept in a room with a controlled temperature (22 °C) and maintained under a 12-h light-dark cycle. The protocol of PRP production and quantification as well as the surgical procedures performed in this study were based on Portela et al. (5) and are described below.

PRP Production and Quantification

An amount of 3.2 mL of autogenous blood was collected from each animal through cardiac puncture into a syringe containing 0.35 mL of 10% sodium citrate. The blood collected from each animal was centrifuged at 200×g for 20 min at room temperature in order to separate the plasma and platelets from the erythrocytes (Beckman J-6M Induction Drive Centrifuge; Beckman Instruments Inc., Palo Alto, CA, USA). The plasma fraction was collected from the top of the supernatant. The remaining portion was centrifuged once more at 400×g for 10 min at room temperature to separate the platelets. The plasma fraction was removed from the upper level of the supernatant, leaving the PRP and buffy coat. Both the buffy coat and PRP (0.35 mL) were re-mixed and activated with a mixture of 10% calcium chloride (0.05 mL/mL of PRP). They were then added to the previously prepared PRP and mixed for 1 min until they formed a gel.

The platelets and leukocytes on the PRP were counted after centrifugation using a Coulter STKS hematology-counting machine (Beckman-Coulter, Chicago, IL, USA).

Surgical Procedure

The rats were anesthetized by intramuscular injection of xylazine (5 mg/kg) and ketamine (70 mg/kg). The surgical region was shaved and aseptically prepared with sterile barriers in order to limit the surgical field. A 5-cm dermo-periosteal incision was made along the midline to expose the calvarium surface with complete removal of the periosteum in order to remove the fibroblast and periosteum stem cells and their possible proliferation into the artificial defect. An artificial defect of 5×1 mm (diameter × depth) was created with a trephine (Biomedical Research Instruments Inc., Silver Spring, MD, USA) under abundant saline solution irrigation in each rat.

Bone fragments removed from each rat's own calvarium were particulated and used as autograft. Particulation of calvarium bone fragment was obtained using an exclusive periodontal instrument for bone particulation developed by Neodent (Curitiba, PR, Brazil). Images of the particles were captured with a digital camera and analyzed with Image J software (National Institutes of Health, Bethesda, MD, USA) to determine the average particle size. An image size of 1 mm was used to standardize all measurements. The average bone particle size of autograft was 0.95±0.03 mm^2.

The animals were randomly assigned to 4 groups (n=14) in which the defects were filled with 0.01 mL of autograft, 0.01 mL of autograft plus 0.15 mL PRP, 0.15 mL of PRP or natural blood clot (sham group). Soft tissues were repositioned and sutured to achieve primary closure (4-0 silk, Ethicon, São Paulo, SP, Brazil). Each animal received a prophylactic intramuscular injection of 24,000 IU of penicillin G benzathine and a daily dose of 200 mg/kg/day of liquid acetaminophen administrated orally.

Euthanasia Procedure and Tissue Processing

On 2nd or 6th week post-surgery (n=7/group) the animals were euthanized by brief exposure in a CO_2 chamber. The calvarium of each animal was necropsied using an inverted cone bur. The fragments obtained were fixed in 10% buffered formalin for 48 h and decalcified in 20% formic acid and sodium citrate for 7 days. The specimens were washed with tap water, dehydrated, cleared in xylene and embedded in paraffin. Serial 3-µm-thick sections parallel to the mid-sagittal suture were cut from the center of each defect using a microtome (RM2155, Leica Microsystems GmbH, Nussloch, Germany) and stained with Giemsa to observe the qualitative and quantitative histological characteristics.

Immunohistochemistry Processing

The specimens were deparaffinized and subjected to antigen retrieval 1% pepsin solution (pH 1.8) for 1 h at 37 °C for all the antibodies. The slides containing the histological pieces were immersed in 3% hydrogen peroxide for 30 min to remove endogenous peroxidase activity, followed by incubation with 1% phosphate-buffered saline (pH 7.4; PBS). The sections were incubated overnight with the primary antibody anti-Erk1/2 (ab17942, 100 µg/mL, peptide corresponding to human Erk1 + Erk2 aa 317-339 of C-terminal sequence (Abcam, Cambridge, UK), with 1:150 dilution; anti-p38α/β (clone A12, sc-7972, 200 µg/ml, C-terminal chain of p38α of human origin) (Santa Cruz Biotechnology, Paso Robles, CA, USA) with 1:100 dilution; anti CD36 (clone V19, sc-7641, 200 µg/ml, N-terminal chain of CD36 of human origin, (Santa Cruz) with 1:50 dilution and anti-Adiponectin (ab22554, 100 µg/mL; (N-terminal peptide, Abcam) with 1:100 dilution. The labeled streptavidin biotin antibody-binding detection system (Universal HRP immunostaining kit; Diagnostic Biosystems, Foster City, CA, USA) was employed to detect the primary antibodies. The immune reaction was revealed with diaminobenzidine tetrachloride chromogen solution (Diagnostic Biosystems), which produced a brown precipitate at the antigen site. The specimens were counterstained with Harris hematoxylin for 30 s. A negative control was made for all samples using rabbit polyclonal isotype IgG (2 µg/mL, Abcam, ab 27472) for 10 min at room temperature as a primary antibody. For each specimen, three slides were used for incubation with each antibody.

Image Analysis

The images of both the histological and immunohistochemistry slices were taken with a digital camera (Samsung, Seoul, South Korea) connected to a light microscope with 200× original magnification. Each digital image was captured and saved with 600 dpi resolution, producing a virtual picture of 115.88×81.93 cm (ou mm?). Because it was not possible to have the entire bone defect in a single image at the used magnification, a digital image of the whole defect was built by combining two smaller images based on reference histological structures.

All histomorphometric measurements were made using the Image J software (National Institutes of Health). The histomorphometric data were quantified manually and expressed as area observed at 5 mm^2. The immunopositivity for Erk1/2, p38α/β, CD36 and adiponectin was determined by automation, as described by Portela et al. (5). All immunohistochemical results were performed in triplicate and all data were transformed into percentages in order to facilitate their interpretation.

Statistical Analysis

Each parameter was evaluated separately within the monitoring period. The significant similarities among all groups were determined by an analysis of variance, followed by Student Newman-Keuls non-parametric test. A $p<0.05$ was considered statistically significant.

Results

Platelet and Leukocyte Counts

For platelets, the average number in the whole blood and in the PRP was $638.62\pm54.12\times10^3$ and $2791.81\pm312.28\times10^3$ platelets/mL, respectively ($p<0.05$). For leukocytes, the average number in the whole blood and in the PRP was $9.07\pm0.32\times10^3$ and $3.01\pm0.71\times10^3$ leukocytes/mL ($p<0.05$).

Light Microscopy Analysis

A concise description of the microscopic characteristics found among groups was performed, while the histomorphometric data were summarized in Figures 1A and 1B.

Autograft: On the 2nd postoperative week, there was granulation tissue (gt) surrounding bone fragments (bg) with new bone formation derived likely from the autograft (Fig. 2A). On the 6th postoperative week, the presence of haversian compact bone (hcb) was evident and the fibrous tissue was scarce and restricted to the well-delimited bone marrow (ma) and/or periosteum (Fig. 2B).

Autograft mixed with PRP: On the 2nd week after surgery, the histological findings were similar to those observed in the group treated with autograft, although autogenous bone (bg) composed by smaller *de novo* bone fragments were present peripherally and they were surrounded by a rich granulation tissue (gt) (Fig. 2C). On the 6th week post-surgery the amount of bone matrix deposited into the defect increased slightly. The largest part of artificial defect was considered as a medullary area (ma) (Fig. 2D) composed by a rich fibrous and dense connective

tissue (ft) and foam-like cells (arrows), surrounding the new blood vessels (bv) (Fig. 2E).

PRP: Histological analysis after the 2nd week post-surgery revealed intense fibrous connective tissue (ft) (Fig. 2F), without evidence of significant new bone formation. On the 6th week, the largest area of defect was represented by intense fibrous tissue (ft) (Figs. 2G and 2H) and presence of adipose-like cells (fc) (Fig. 2H).

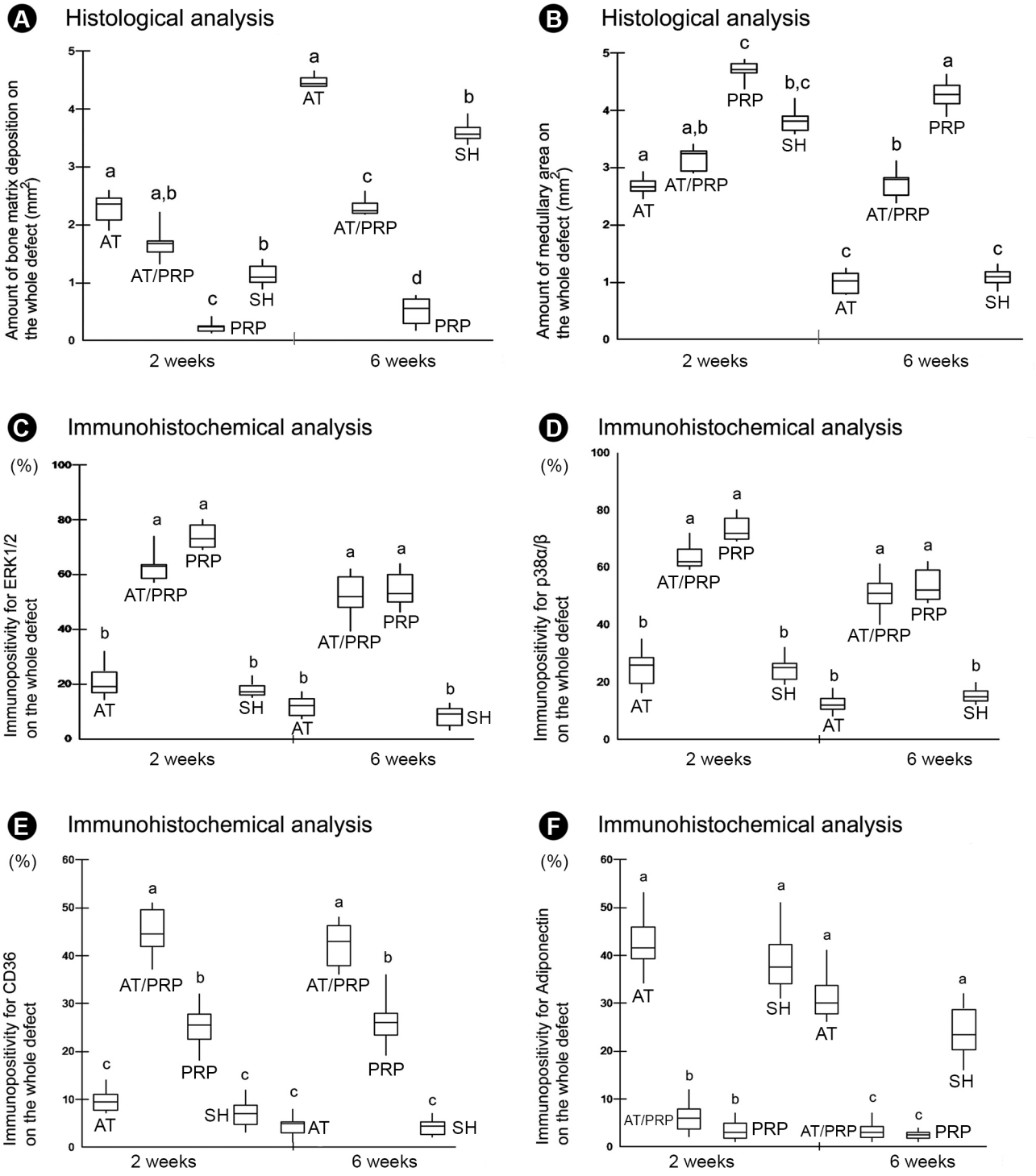

Figure 1. Box plot diagrams representing the histological and immunohistochemical results of the groups. The median, maximum and minimum values of the amount (mm^2) of bone matrix deposition and medullary area in each group are presented in panels A and B, respectively. The median, maximum and minimum percent values of Erk1/2, p38α/β, CD36 and adiponectin expression in each group are presented in panels C, D, E and F, respectively. Values followed by the same superscript letter are statistically similar ($p>0.05$). AT= autograft; AT/PRP = autograft mixed to PRP; PRP= only PRP; SH=sham.

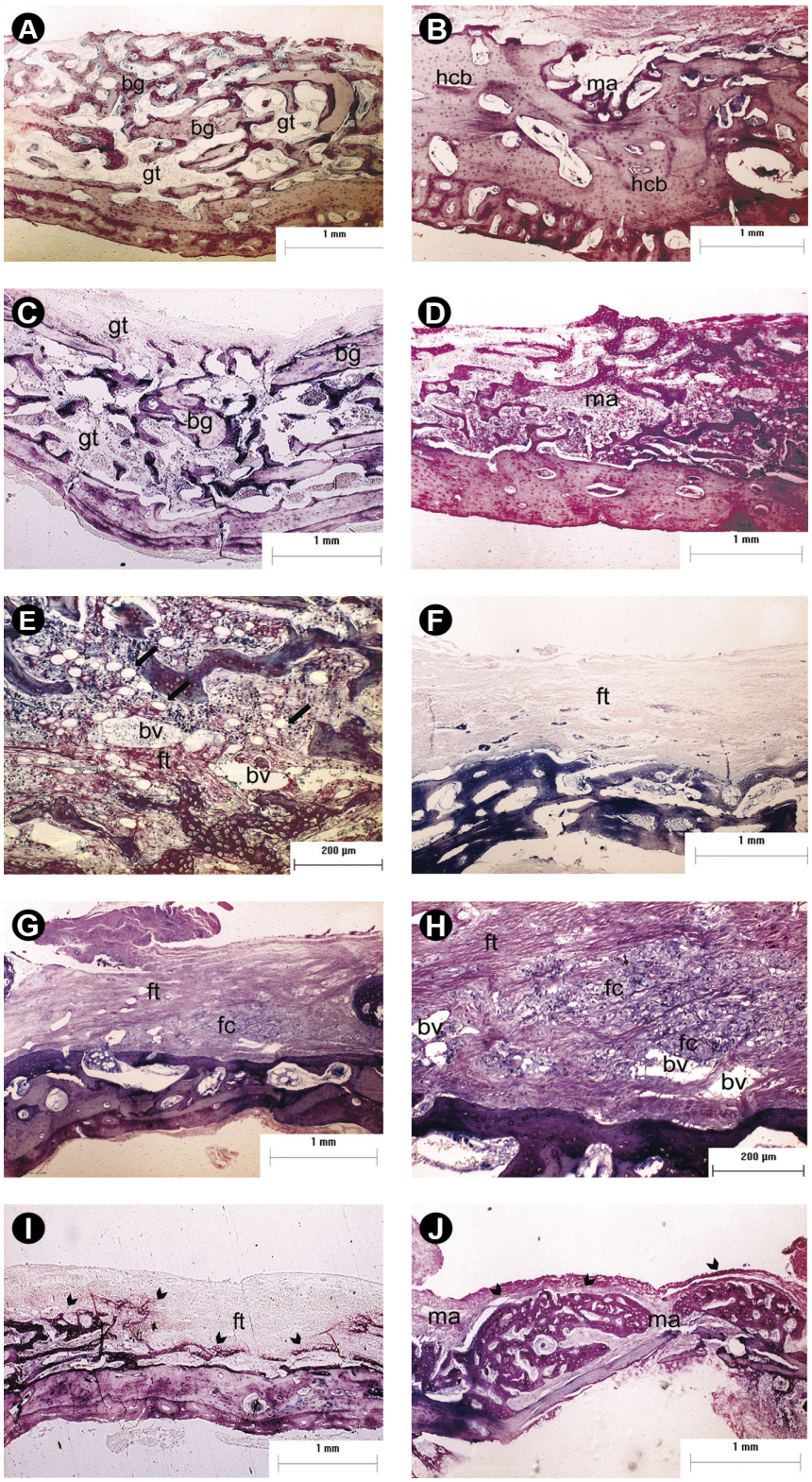

Figure 2. Histological characteristics observed in each group. Panels A and B represent specimens treated with autograft. "A" shows the bone graft (bg) surrounded by granulation tissue (gt) on the 2nd week post-surgery and "B" shows an intense haversian compact bone (hcb) in the artificial defect on the 6th week post-surgery. Panels C, D and E represent specimens treated with autograft +PRP. "C" shows the bone graft (bg) and intense presence of granulation tissue (gt) on the 2nd week post-surgery, "D" shows an intensive atherofibrotic area composing the medullary area (ma) on the 6th week post-surgery, and "E" shows atherofibrotic features, with foam-like cells (arrows) surrounding the new blood vessels (bv). Panel F shows the fibrotic area (ft) developed in the group treated PRP on the 2nd week post-surgery. Similar aspect was observed on the 6th week post-surgery, where it is possible to see intense fibrosis (ft) and foam-like cells in panoramic view (panel G) and in detail (panel H). Panels I and J represent specimens of the sham group. "I" shows fibrous tissue (ft) and bone matrix (chevron) developed on the 2nd week post-operative, and "J" shows greater bone matrix deposition (chevron) surrounding the fibrotic area considered as a medullary area (ma). Giemsa staining. Original magnifications 40× (A, B, C, D, F, G, I, J) and 200× (E and H).

No treatment (Sham): On the 2nd week post-surgery, areas of fibrous tissue (ft) were present in the larger part of the defect, however the presence of new bone formation (chevron) was evident (Fig. 2I). On the 6th postoperative week, a well-developed cancellous bone composed of both mature and immature tissue (chevron) was observed (Fig. 2J).

Immunohistochemistry Analysis

Erk1/2

All groups exhibited positivity to Erk1/2 and the measurements for each group can be seen in the Figure 1C. On the 2nd week, scarce positive Erk1/2+ cells were observed on the PRP-free groups, especially surrounding the blood vessels in the sham group (Fig.3 G) or scarce cells surrounding the autograft (bg) (Fig. 3A). The amount of positivity for Erk1/2 remained low on the 6th week post-surgery. The immunopositivity was restricted to the medullar area in both autograft group (Fig. 3B) and sham (Fig. 3H) groups. In contrast, intensive and diffuse deposition of Erk1/2+ cells and ECM was observed spread in the defects of the PRP groups. In specimens that received only PRP, the pattern of distribution and number of positive cells to Erk1/2 were similar on the 2nd (Fig. 3E) and 6th (Fig. 3F) weeks. The immunopositivity was prevalent in cells that composed the fibrotic EMC (ft). In specimens treated with autograft combined with PRP, a large number of cells of fibrotic ECM (ft) were positive for Erk1/2, while on the 6th week post-surgery the prevalent cells were foam-like cells and fibrocytes surrounding the new blood vessels (bv).

p38α/β

The pattern of distribution of p38α/β+ was similar to that of Erk1/2. All groups exhibited positivity to p38α/β+ and their amounts are shown in Figure 1D. On the 2nd week post-surgery, few positive p38α/β+ cells were found on the PRP-free groups. They were spread in the granulation (gt) or fibrous tissue (ft), on the sham group (Fig. 4G) or concentrated peripherally to bone graft (bg) in the autogenous group (Fig. 4A). The pattern on the 6th postoperative week remained similar to that observed in the 2nd week post-surgery, but most of the positivity was found in the medullar area (ma) or concentrated around the new bone formation (nbf) as illustrated in Figure 4B (autograft group) and Figure 4H (sham group). Differently, significant positivity for p38α/β+ was seen diffusely in the defects in the PRP groups. In specimens treated with PRP only, the distribution pattern and amount of positivity for p38α/β+ was similar in the 2nd (Fig. 4E) and 6th (Fig. 4F) weeks in the cells and ECM (ft) that compose the larger portion of the reparative area. In specimens treated with autograft mixed to PRP, a large number of cells surrounding the bone graft (bg) was positive for p38α/β+, while on the 6th week post-surgery the prevalent p38α/β+ cells were foam-like cells and/or fibrocytes surrounding the new blood vessels (bv).

CD36

All specimens were positive to CD36 as the pattern exhibited in Figure 1E. On 2nd week post operative the presence of CD36 was restricted in the area surrounding the blood vessels (arrows) (Fig. 5A), while to 6th week, the pattern was similar, however the majority of CD36 was seen in medullar area, especially in the autograft group (Fig. 5B). The immunopositivity for CD36 (arrows) was diffuse in groups that received PRP. They were observed in cells that compound the granulation tissue on 2 weeks post surgery (Fig. 5C) and especially in foam-like cells (arrows) that surrounded the blood vessels (bv) on 6th week post surgery, both in the group treated with autograft (Fig. 5D) and the one treated with PRP (Fig. 5E) only.

Adiponectin

On the 2nd week post-surgery there was a positive immunostaining to adiponectin in all groups (Fig. 1F), but it was significantly weaker in the groups that received PRP compared with the PRP-free groups. On the 2nd week post-surgery, the positivity was found surrounding the autograft (bg) (arrow) (Fig. 6B) or spread on the fibrous tissue (ft) (Fig. 6E). On the 6th postoperative week, the immunopositivity decreased as soon as the medullar area or fibrosis (ft) was deposited in the defect (Figs. 6D and 6F). In the autograft group, the immunopositivity was intense on the 2nd week post surgery, both in the fibrous tissue (ft) deposited in the defect (Fig. 6G) and occupying all space peripheral to bone graft (bg) (Fig. 6A). The pattern of adiponectin was the same on the 6th week post-surgery, but the amount decreased as soon as the bone matrix (nbf or hcb) was formed (Figs. 6B and 6H).

Discussion

The present study showed an increase in Erk1/2, p38α/β and CD36 immunohistochemical expression concomitant with a significant decrease in the immunopositivity for adiponectin in the specimens that received PRP. These finding coincided with the prevalent deposition of adipose-fibrotic tissue while the bone matrix formation was scarce.

The presence of fibrosis in reparative sites treated with PRP has been previously reported (16) and there are two hypotheses that may explain this result. The first hypothesis is based especially on the presence of platelets and its thrombogenic-like effect. It is known that platelets have a specific receptor for the different types of collagen (I, III

and IV). Changes in collagen type and distribution patterns on repair sites would contribute to the development of fibrosis, which is totally different from the development of bone tissue, rich only in collagen type I (17). The second hypothesis suggests that the greater synthesis of a platelet growth factor (TGF-β1) may induce the formation of actin myofilaments in the cells that compose the reparative sites, a fact that also contributes to the occurrence of

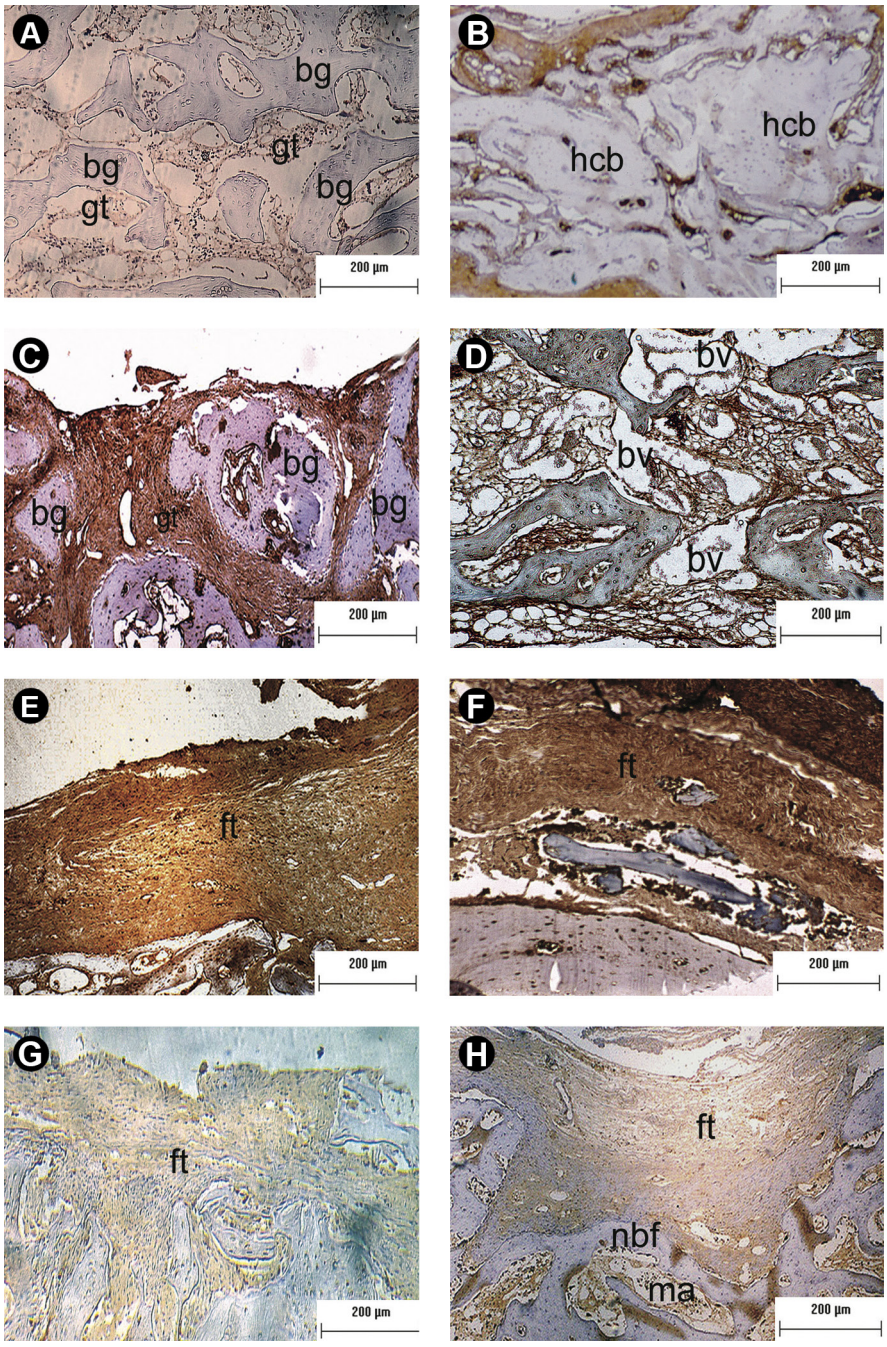

Figure 3. Immunopositivity for Erk1/2. Panels A and B show, respectively, the pattern of Erk1/2 immunoexpression on the 2nd and 6th week post-surgery in specimens treated with autograft. Verify the scarce number of Erk1/2+ cells concentrated in the granulation tissue (gt) around the bone graft (bg) on the 2nd week, and presence of Erk1/2+ cells in the medullary area surrounded by haversian compact bone (hcb) on the 6th week. Panels C and D show intense positivity in the specimens treated with autograft+PRP on the 2nd and 6th week post-surgery, respectively. "C" shows the presence of protein surrounding the bone graft (bg) on the 2nd week, while "D" reveals the presence of Erk1/2 in areas of fibrosis and foam cells surrounding the new blood vessels (bv). Panels E and F show, respectively, the pattern of Erk1/2 immunoexpression on the 2nd and 6th week post-surgery in specimens treated with PRP. There is intense presence of Erk1/2 in the fibrous tissue (ft) in both periods. Panels G and H show, respectively, the pattern of Erk1/2 immunoexpression in the sham group. "G" shows scarce presence of protein on the 2nd week, while H reveals the presence of Erk1/2 especially in medullary area (ma) and scarce in fibrous tissue (ft) on the 6th week (Original magnification ×100).

pathological fibrosis (4).

The coexistent immunohistochemical expression of CD36, p38 and Erk1/2 in specimens treated with PRP not only supports these two hypotheses of fibrosis, but also indicates that these events seem to be interdependent. Our suggestion is supported by the hypothesis that the expression of anchorage molecules, like thrombospondin receptor-CD36, only occurs when platelets are exposed

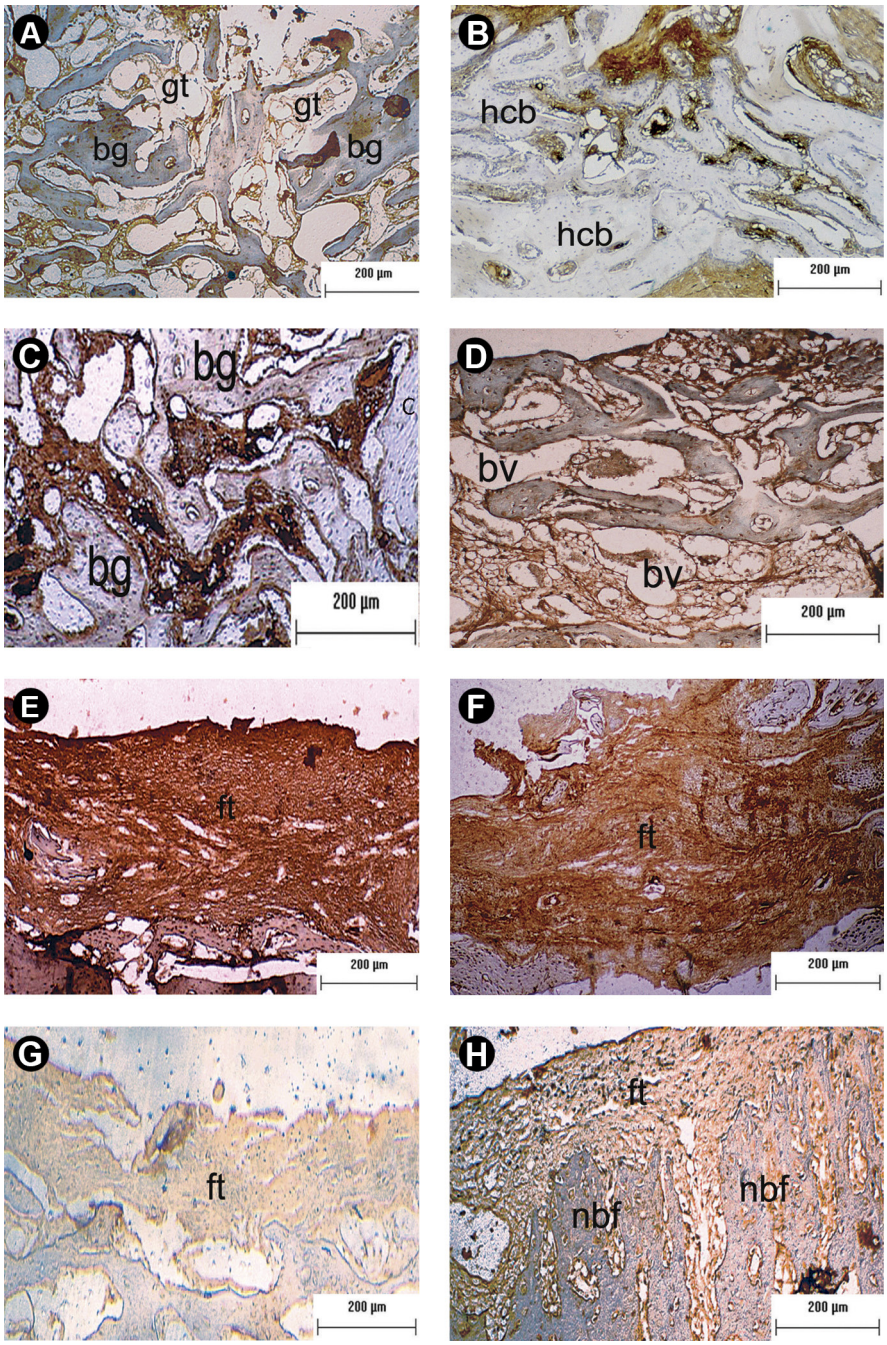

Figure 4. Immunopositivity for p38α/β Panels A and B show, respectively, the pattern of p38α/β immunoexpression on the 2nd and 6th week post-surgery in specimens treated with autograft, respectively. There is discrete presence of protein in the cells of the granulation tissue (gt) around bone graft (bg) on the 2nd week and in the well-formed medullary area surrounded by haversian compact bone (hcb) on the 6th week. Panels C and D show intense positivity in the specimens treated with autograft+PRP on the 2nd and 6th week post-surgery, respectively. "C" shows the presence of protein surrounding the bone graft (bg), while "D" shows the presence of fibrotic and foam cells positive for p38α/β surrounding the new blood vessels (bv). Panels E and F show, respectively, the pattern of p38α/β immunoexpression on the 2nd and 6th week post-surgery in specimens treated with PRP, respectively. There is intense presence of p38α/β in the fibrous tissue (ft) in both periods. Panels G and H show, respectively, the pattern of p38α/β immunoexpression in the sham group. "G" shows scarce presence of protein on the 2nd week, while H reveals the presence of p38α/β especially in medullary area (ma) and scarce in the fibrous tissue (ft) on the 6th week. (Original magnification 100×).

to collagen or ECM proteins (18). The signaling, initiation and expression of adhesive proteins for these interactions are driven by fibrin and von Willembrand factor (vWF) by stimulation and expression of p38 protein. The importance of p38 in the thrombogenesis seems to be crucial and it is supported in the previous study that evaluated the role of p38 in platelet activation, and platelet-collagen interaction applying a p38-inhibitor (SB203580) (19). When the p38-inhibitor was used, both platelet aggregation and its interaction with ECM were suppressed, results that strictly indicated that the p38 plays an important role in the platelet during the thrombogenesis (13).

Yet, there are lines of evidence that demonstrate that the p38 also contributes to fibrosis. Pichon et al. (20) described that p38 expression is required for control of cytoskeleton reorganization and actin polymerization when induced by the platelet growth factor TGF-β1. It supports the hypothesis that in fact the PRP may induce thrombogenesis at the same time that it may induce fibrosis, as demonstrated here in the histological analysis.

Conversely, it is noteworthy that the modulation of the platelet response to ECM occurs directly or indirectly by the 2-site-2-step model (21). This viewpoint is elucidated in models of thrombus formation and tissue regeneration produced in vessel wall damage. In some conditions, the platelets adhere directly via collagen receptor and this adhesion depends on p38. On the other hand, under stress condition, collagen fibers are exposed and platelets initially interact via glycoprotein Ib-V-IX and vWF bound to collagen. This peculiar pathway depends on Erk1/2 (22).

The co-expression between Erk1/2 and p38 in the thrombogenesis has also been highlighted by Li et al. (23), who revealed that the presence of p38 is required for activation of Erk1/2 pathway, while Flevaris et al. (22) demonstrated *in vitro* that the presence of Erk1/2 is crucial in the activation of the platelet granule secretion for growth factor release.

At the same time that presence of Erk1/2 may contribute indirectly to fibrous deposition in repair sites, the presence of this kinase also seems to be a trigger to impair ECM

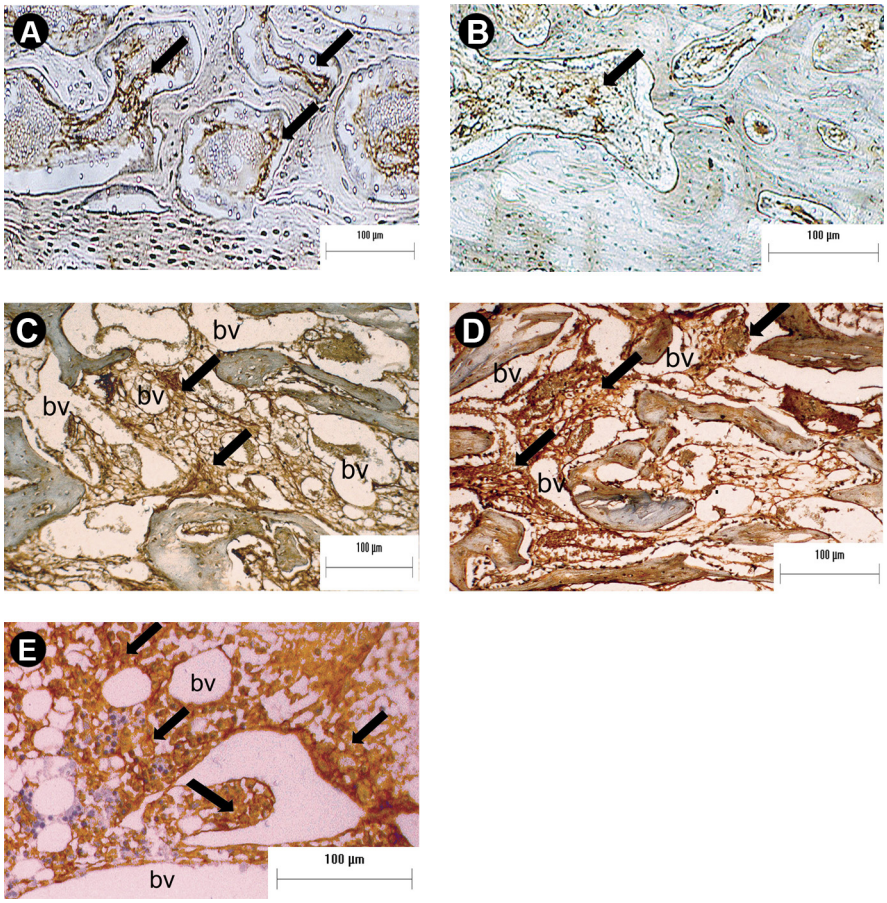

Figure 5. Immunopositivity for CD36. Panels A and B reveal the scarce positivity (arrows) in the PRP-free groups on the 2nd and 6th weeks post-surgery, respectively. Panels C and D show the intense positivity for CD36 in the autograft+PRP group on the 2nd and 6th weeks post-surgery, especially in foam cells surrounding the blood vessels (bv). Panel E shows the pattern of CD36 expression in the cellular membrane of foam cells (arrows), characterizing the atherofibrotic aspect around the blood vessels (bv) in specimens treated with only PRP on the 6th week post-surgery (Original magnifications 200× (for Figures A, B, C and D) and 400× (E).

mineralization. Kono et al. (24) demonstrated both *in vivo* and *in vitro* that the immunopresence of Erk1/2 negatively regulates osteoblast differentiation and mineralization. For this conclusion, those authors verified that under a direct induction of Erk1/2, the genetic expressions of BMP-2 and ALP were significantly inhibited, fact that was not verified in specimens where the Erk1/2 was suppressed. This hypothesis may be confirmed, since there is scarce presence of OC in the specimens treated with PRP. The interpretation of these results suggests that the PRP works in order to mimic a physiological action of platelets, which are the main factors responsible for remodeling of intimae and media vascular tunicae at the same time trying to protect the regenerative tissue against the pathological mineralization.

However, the persistent expression of CD36 in specimens treated with PRP deserves attention and give evidences that this cluster of differentiation may be not only associated to collagen/ECM-platelets interaction, but it may also

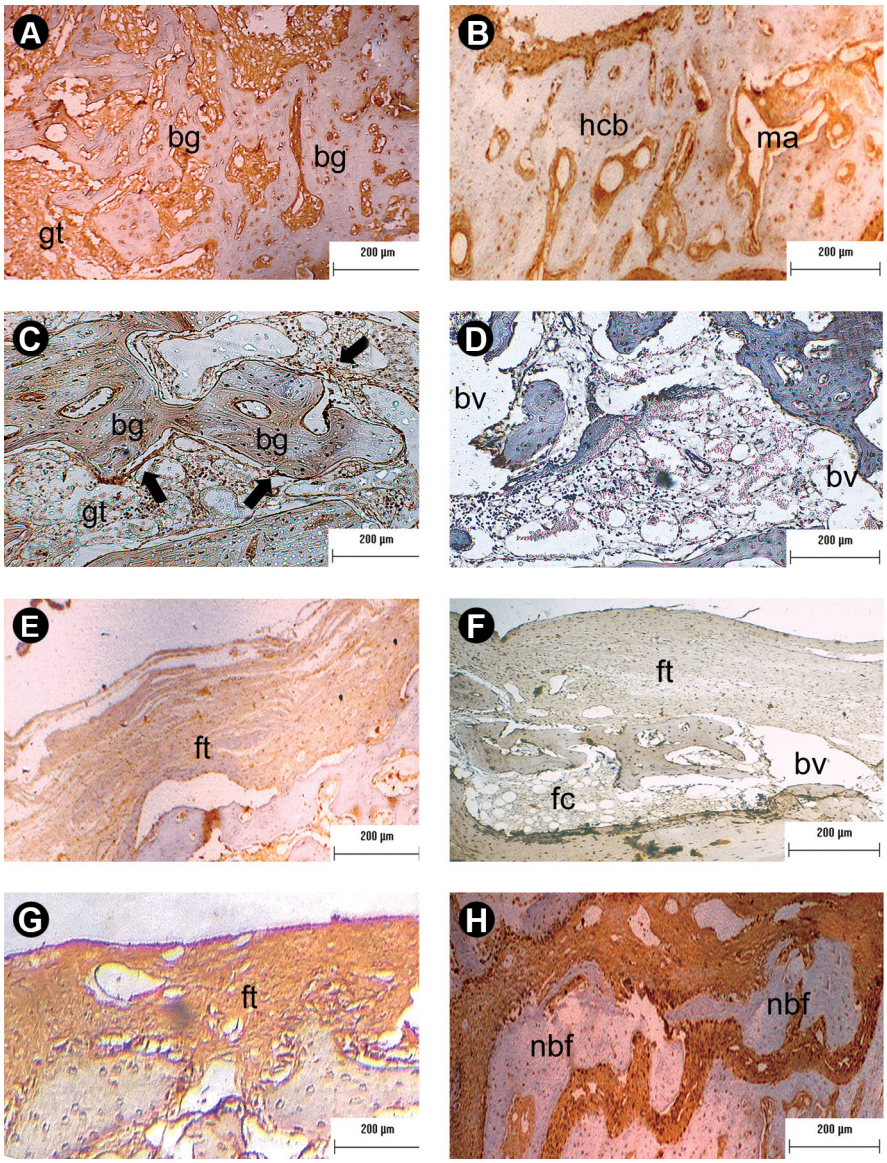

Figure 6. Immunopositivity for adiponectin. Panels A and B show, respectively, the pattern of adiponectin immunoexpression on the 2nd and 6th week post-surgery in specimens treated with autograft, respectively. There is intense presence of adipoprotein in the cells of the granulation tissue (gt) that surrounding bone graft (bg) on the 2nd week and in the well-formed medullary area surrounded by haversian compact bone (hcb) on the 6th week. Panels C and D show scarce positivity in the specimens treated with autograft+PRP on the 2nd and 6th week post-surgery, respectively. "C" shows the presence adipoprotein concentrated only in cells (arrows) in close contact with bone graft (bg), while "D" shows the lack of positivity for adiponectin in foam cells that surrounding the new blood vessels. Panels E and F show, respectively, the pattern of adiponectin immunoexpression on the 2nd and 6th week post-surgery in specimens treated with PRP, respectively. Verify the discrete presence of adiponectin in the fibrous tissue (ft) in both periods. Panels G and H show, respectively, the pattern of adiponectin immunoexpression on the 2nd and 6th week post-surgery in the sham group. "G" shows significant presence of protein on the 2nd week, while "H" reveals the presence of adiponectin especially surrounding the new bone formed in defect (nbf) on the 6th week. (Original magnification ×100).

contribute to development of foam cells. This hypothesis derives from the premise that the class B scavenger receptor CD36 also acts as a fatty acyl translocase protein responsible for recognition and internalization of oxidatively modified low-density lipoprotein (oxLDL) in several types of cells including hematopoietic cells, monocytes, macrophage, adipocytes and vascular cells that include endothelium and smooth muscle cells (8).

Since intracellular oxLDL works as a nuclear transcription factor for expression of CD36 scavenger receptor, it is acceptable the hypothesis that intense CD36+ platelets are associated to foam-like cells development (25). However, the co-occurrence of CD36 and other biological condition that act in disruption of intracellular/extracellular flux of oxLDL is crucial and required for dyslipidemia (26).

Here we suggested that the significant decrease of immunohistochemical expression of adiponectin could be an important factor to foam cell-like development when PRP is used. This hypothesis is supported by previous studies that attribute to adiponectin the hallmark of the initiation and development of the dyslipidemic pathological conditions including atherosclerosis. In these pathological conditions, lack of adiponectin expression commonly occurs, especially in the membrane of monocytes and macrophages, a result that contrasts with the usual situation that commonly reveals positivity for adiponectin in cells where the efflux of cholesterol occurs (27). The real reason of decreased adiponectin expression found here remains unclear, but a supposition that should be considered to explain our findings is the removal of plasma during PRP fabrication. Our inference is feasible since the adiponectin constitutes an important a plasmatic protein.

Additionally, the lack of significant expression of adiponectin also may be another piece of information that could help explaining not only the atherofibrotic histophenotype produced in specimens treated with PRP, but also the impairment of bone matrix formation in this study. According to these hypotheses, Thomas et al. (28) observed positivity for alkaline phosphatase and BMP-2 in osteoprogenitor cells culture when adiponectin was administrated. Similarly, Kanazawa et al. (15) indicated that adiponectin and its expression is involved in proliferation, differentiation and mineralization of osteoblastic cells since this adipokine indirectly works as a transcription factor for osteorix mRNA expression. On the other hand, the negative correlation between adiponectin expression and fibrogenesis was demonstrated in the scleroderma, suggesting a potential role for adiponectin in the pathogenesis of fibrosis. This hypothesis is supported by results that demonstrated that both RNA-i mediated adiponectin knockdown in normal fibroblast and genetic depletion of adiponectin in mouse fibroblast revealed increase of smooth-actin muscle intracellular filaments as well as increase of collagen deposition (14).

In conclusion, it was demonstrated in the present study that the treatment of bone defects with PRP impaired bone matrix formation and induced an atherofibrotic histophenotype. These results were concomitant with the increase of Erk1/2 and p38α/β co-expression and an intense presence of cells that exhibit scavenger receptor CD36+/adiponectin-.

Resumo

A interação da matriz extracelular-plaquetas no plasma rico em plaquetas (PRP) através de receptor trombospondina CD36 induz a secreção de fatores de crescimento responsáveis pela proliferação e diferenciação celular durante o processo de reparo. Uma vez que o CD36 também age como receptor *scavenger* de classe B para o desenvolvimento de células do tipo espuma, e as quinases ativadas por mitógenos, tais como ERK1/2 e p38α/β, são importantes proteínas ativadas por fator de crescimento das plaquetas, o objetivo deste estudo foi avaliar a presença imunoistoquímica de CD36, ERK1/2, p38α/β durante o reparo ósseo tratado e não-tratado com PRP e comparar estes resultados com a histomorfometria do reparo. Simultaneamente, analisou-se a imunopresença da adiponectina, que pode contribuir para osteogênese ao mesmo tempo que inibe a fibrose e prejudica a formação de células tipo espuma/xantomatosas na área medular. Um defeito artificial de osso medindo 5×1 mm foi produzido na calvária de 56 ratos Wistar. Os defeitos foram tratados aleatoriamente com auto-enxerto, enxerto autógeno+PRP, PRP apenas e sham. Os animais foram sacrificados 2 e 6 semanas pós-cirurgia. Os dados foram examinados por meio de ANOVA, seguido pelo teste não-paramétrico Student Newman-Keuls (p<0,05) para a interpretação histomorfométrica e imunoistoquímica. Os resultados revelaram que as amostras que receberam PRP aumentaram significativamente a imunopositividade para as proteínas ERK1/2, p38α/β e CD36, simultaneamente à diminuição de expressão imunoistoquímica da adiponectina. Houve também expressiva redução de deposição de matriz óssea e aumento da área medular representada por fibrose e/ou presença de células do tipo espuma que apresentaram imunofenótipo CD36 + adiponectina. Estes resultados sugerem que o PRP atuou como um inibidor da osteogênese durante o reparo ósseo craniofacial e induziu uma condição patológica que mimetiza uma condição aterofibrótica.

References

1. Marx RE, Carlson ER, Eichstaedt RM, Schimmele SR, Strauss JE, Georgeff KR. Platelet-rich plasma: Growth factor enhancement for bone grafts. Oral Surg Oral Med Oral Pathol Oral Radiol Endod 1998;85:638-646.
2. Freymiller EG, Aghaloo TL. Platelet-rich plasma: ready or not? J Oral Maxillofac Surg 2004;62:484-488.
3. Aghaloo TL, Moy PK, Freymiller EG. Evaluation of platelet-rich plasma in combination with anorganic bovine bone in the rabbit cranium: a pilot study. Int J Oral Maxillofac Implants. 2004,19:59-65.
4. Giovanini AF, Gonzaga CC, Zielak JC, Deliberador TM, Kuczera J, Göringher I, et al.. Platelet-rich plasma (PRP) impairs the craniofacial bone repair associated with its elevated TGF-beta levels and modulates the co-expression between collagen III and alpha-smooth muscle actin. J Orthop Res 2011;29:457-463.
5. Portela GS, Cerci DX, Pedrotti G, Araujo MR, Deliberador TM, Zielak JC, et al.. L-PRP diminishes bone matrix formation around autogenous bone grafts associated with changes in osteocalcin and PPAR-gamma immunoexpression. Int J Oral Maxillofac Surg 2014;43:261-268.
6. Roberts DE, McNicol A, Bose R. Mechanism of collagen activation in human platelets. J Biol Chem 2004;279:19421-19430.
7. Daub K, Langer H, Seizer P, Stellos K, May AE, Goyal P, et al.. Platelets induce differentiation of human CD34+ progenitor cells into foam cells and endothelial cells. FASEB J 2006;20:2559-2561.

8. Silverstein RL, Li W, Park YM, Rahaman SO. Mechanisms of cell signaling by the scavenger receptor CD36: implications in atherosclerosis and thrombosis. Trans Am Clin Climatol Assoc 2010;121:206-220.
9. Allori AC, Sailon AM, Warren SM. Biological basis of bone formation, remodeling and repair-part II: extracellular matrix. Tissue Eng Part B Rev 2008;14:275-283.
10. Han MY, Kosako H, Watanabe T, Hattori S. Extracellular signal-regulated kinase/mitogen-activated protein kinase regulates actin organization and cell motility by phosphorylating the actin cross-linking protein EPLIN. Mol Cell Biol 2007;27:8190-8204.
11. Chang L, Karin M. Mammalian MAP kinase signalling cascades. Nature 2001;410:37-40.
12. Xu DJ, Zhao YZ, Wang J, He JW, Weng YG, Luo JY. Smads, p38 and ERK1/2 are involved in BMP9-induced osteogenic differentiation of C3H10T1/2 mesenchymal stem cells. BMB Rep 2012;45:247-252.
13. Saklatvala J, Rawlinson L, Waller RJ, Sarsfield S, Lee JC, Morton LF, et al.. Role for p38 mitogen-activated protein kinase in platelet aggregation caused by collagen or a thromboxane analogue. J Biol Chem 1996;271:6586-6589.
14. Fang F, Liu L, Yang Y, Tamaki Z, Wei J, Marangoni RG, et al.. The adipokine adiponectin has potent anti-fibrotic effects mediated via adenosine monophosphate-activated protein kinase: novel target for fibrosis therapy. Arthritis Res Ther 2012;14:R229.
15. Kanazawa I, Yamaguchi T, Yano S, Yamauchi M, Yamamoto M, Sugimoto T. Adiponectin and AMP kinase activator stimulate proliferation, differentiation, and mineralization of osteoblastic MC3T3-E1 cells. BMC Cell Biol 2007;8:51.
16. Cerci DX, Portela GS, Cunha EJ, Grossi JR, Zielak JC, Araújo MR, et al.. Leukocyte-platelet-rich plasma diminishes bone matrix deposition in rat calvaria treated with autograft due to simultaneous increase in immunohistochemical expression of Indian Hedgehog, transforming growth factor-β, and parathyroid-1 receptor. J Craniomaxillofac Surg 2015;43:1470-1477.
17. Giovanini AF, Deliberador TM, Gonzaga CC, de Oliveira Filho MA, Göhringer I, Kuczera J, et al.. Platelet-rich plasma diminishes calvarial bone repair associated with alterations in collagen matrix composition and elevated CD34+ cell prevalence. Bone 2010;46:1597-1603.
18. Jarvis GE, Atkinson BT, Snell DC, Watson SP. Distinct roles of GPVI and integrin alpha(2)beta(1) in platelet shape change and aggregation induced by different collagens. Br J Pharmacol 2002;137:107-117.
19. Canobbio I., Reineri S, Sinigaglia F, Balduini C, Torti M. A role for p38 MAP kinase in platelet activation by von Willebrand factor. Thromb Haemost 2004;91:102-110.
20. Pichon S, Bryckaert M, Berrou E. Control of actin dynamics by p38 MAP kinase - Hsp27 distribution in the lamellipodium of smooth muscle cells. J Cell Sci 2004;117:2569-2577.
21. Nieswandt B, Watson SP. Platelet-collagen interaction: is GPVI the central receptor? Blood 2003;102:449-461.
22. Flevaris P, Li Z, Zhang G, Zheng Y, Liu J, Du X. Two distinct roles of mitogen-activated protein kinases in platelets and a novel Rac1-MAPK-dependent integrin outside-in retractile signaling pathway. Blood 2009;113:893-901.
23. Li Z, Zhang G, Feil R, Han J, Du X. Sequential activation of p38 and ERK pathways by cGMP-dependent protein kinase leading to activation of the platelet integrin alphaIIb beta3. Blood 2006;107:965-972.
24. Kono SJ, Oshima Y, Hoshi K, Bonewald LF, Oda H, Nakamura K, et al.. Erk pathways negatively regulate matrix mineralization. Bone 2007;40:68-74.
25. Munday AD, Gaus K, López JA. The platelet glycoprotein Ib-IX-V complex anchors lipid rafts to the membrane skeleton: implications for activation-dependent cytoskeletal translocation of signaling molecules. J Thromb Haemost 2010;8:163-172.
26. Tian L, Luo N, Klein RL, Chung BH, Garvey WT, Fu Y. Adiponectin reduces lipid accumulation in macrophage foam cells. Atherosclerosis 2009;202:152-161.
27. Wang M, Wang D, Zhang Y, Wang X, Liu Y, Xia M. Adiponectin increases macrophages cholesterol efflux and suppresses foam cell formation in patients with type 2 diabetes mellitus. Atherosclerosis 2013;229:62-70.
28. Thomas DM, Hards DK, Rogers SD, Ng KW, Best JD. Insulin receptor expression in bone. J Bone Miner Res 1996;11:1312-1320.

Received December 17, 2015
Accepted April 18, 2016